

Rotation of ^{92}Nb nucleus about different principal axes

Nidhi Goel^{1,*}, Somnath Nag¹, R. Palit², Md. S.R.Laskar², F.S.Babra², P. Dey², Biswajit Das², Abraham T Vazhappilly², S. Jadhav², and B. S. Naidu²

¹Dept. of Physics, Indian Institute of Technology (BHU), Varanasi (U.P.), India and

²Department of Nuclear and Atomic Physics,

Tata Institute of Fundamental Research, Mumbai 400005, India

Introduction

It is well known that the low-lying states in the nuclei around the closed-shell (in the present work $Z \simeq 40$ and $N \simeq 50$) have been dominated by shell model type excitations. On the other hand, the high-spin states of nuclei near closed shells (in $A \sim 90$ and 140) has developed considerable interest in terms of collectivity via rotation of nucleus about the classically unfavored longest principal axis. However, triaxiality in nucleus plays a leading role in determining the possibility of rotation around any of the three principal axes. The energy of rotation around the shortest principal axis becomes favourable for $\gamma \sim 30^\circ$, rotation around the intermediate axis becomes energetically favourable for $\gamma \sim -30^\circ$ and that around the longest axis is around $\gamma \sim -80^\circ$.

In this mass region, regular magnetic dipole band structures with very weak or completely suppressed $E2$ crossovers have been observed at high spins (see example of ^{89}Zr [1]). These bands are generated through rotation of nucleus about the possible longest axis. On the contrary, these are akin to the $E2$ bands in mass 140 region [2]. The configurations of high-spin bands are mostly dominated by protons excitations to higher orbitals, and the excitation of the neutrons across the $N = 50$ neutron core into the next major oscillator shell. In this paper we discuss about the confirmation of spin and parity of different newly observed states by Zheng *et al.* [3] and interpretation of the dipole bands in terms of

rotations about various axes.

Experimental Details

High-spin states in the ^{92}Nb have been populated using the reaction $^{80}\text{Se}(^{18}\text{O}, p5n)^{92}\text{Nb}$ at a beam energy of 99 MeV. The ^{18}O beam from 14UD pelletron accelerator was bombarded on 1.4 mg/cm^2 ^{80}Se with a backing of 1.5 mg/cm^2 ^{27}Al . The γ -rays were detected with the Indian National Gamma Array (INGA) at TIFR. In the present work, three clover detectors each were kept at 157° , 140° , two at 115° , four at 90° , and one detector at 65° with respect to the beam direction. The data were sorted using an offline analysis code MARCOS to generate γ - γ matrix and γ - γ - γ cube [4]. The software package "RADWARE" was used for offline analysis of data [5]. To obtain information on the multipolarity of γ - rays, two asymmetric matrices were built. The first one includes the events detected in detectors at 157° on one axis and those detected in all detectors on the other axis, whereas the second matrix consists of counts registered in detectors at 90° on one axis and those in all detectors on the other axis. The intensity ratio $R_\theta = \frac{I_\gamma(\gamma^{157^\circ}, \gamma^{2^{all}})}{I_\gamma(\gamma^{90^\circ}, \gamma^{2^{all}})}$ distinguishes between the stretched dipole ($\simeq 0.7$) and quadrupole ($\simeq 1.4$) transitions respectively when gated on quadrupole transition. Clover detectors facilitates the linear polarization measurement studies of EM radiation. The polarization asymmetric parameter Δ_{assym} is positive and negative for electric and magnetic transitions respectively. The parameter is defined as $\frac{aN_\perp - N_\parallel}{aN_\perp + N_\parallel}$ where N_\perp and N_\parallel are the number of scattered photons in direction perpendicular and parallel to the direction of reaction plane respectively. The correc-

*Electronic address: nidhi.goel.rs.phy18@itbhu.ac.in

tion factor a as a function of γ energy comes out to be 1.00(5).

Results and Discussion

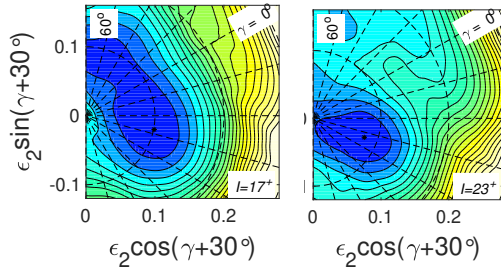


FIG. 1: Total energy surfaces with the constraint, $\pi = +$, $\alpha = 0$. The contour line separation is 0.25 MeV.

We observed most of the transitions as reported by Zheng *et al.* [3]. In addition to already known gamma only a very few new transitions were observed extending the level scheme tentatively up to excitation energy of 11 MeV and $I \sim 22\hbar$. The tentatively assigned spin and parity for all the previously reported new transitions were confirmed. The same will be displayed during the presentation. Zheng *et al.* have assigned configurations to the states in the framework of shell model calculations. Pairing independent cranked Nilsson Strutinsky calculations (CNS) helps in nurturing the collective properties of a nucleus. CNS calculations were performed with parameters derived for $A = 80$ region [6]. For details of calculation please refer to [2, 7]. The Fig. 1 shows the potential energy surfaces as a function of deformation parameters ϵ_2 and γ . For low spin states up to $13\hbar$ the shape is stabilized with $\gamma \sim -10^\circ$ and $\epsilon_2 \sim 0.01$. Upto spin $17\hbar$ the shape shows collective behaviour with $\gamma \sim -43^\circ$, $\epsilon_2 \sim 0.01$ which further collapses to non-collective oblate for higher spin states up to $I \sim 21\hbar$. Beyond $23\hbar$, the energy minimum shifts towards $\gamma \sim -50^\circ$ which signifies probable rotation of the nucleus around the longest principal axis (The state $I \sim 23\hbar$ was not observed till date). Observed excitation energy w.r.t. a liquid drop was plotted as a function of spin (Fig. 2). The same is compared with the calculated re-

sults for a few selected configurations. From the plot, it is concluded that configuration [3, 9] can be assigned to band with configuration $\pi(1g_{9/2}^3) \otimes \nu(1g_{9/2}^{-1}(1g_{7/2}^1)(2d_{5/2}^1))$. For the given configuration, triaxial parameter γ transits from negative value angle $\gamma \sim -53^\circ$ at spin 17 to $\gamma \sim -78^\circ$ at spin 23. Thus, the nucleus can be regarded as an example where we can observe transition of rotating nuclei about a given principal axis to another one.

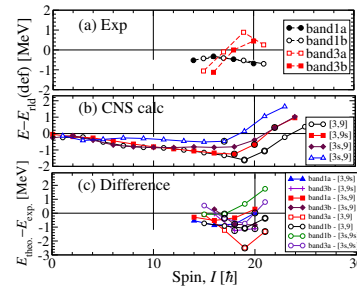


FIG. 2: (a) Experimental excitation energy w.r.t. spin for ^{92}Nb . (b) Calculated excitation energy vs spin for negative parity bands. (c) Comparison of experimental and calculated excitation energies as a function of spin.

Acknowledgement

N.G. acknowledges MHRD for financial support. The authors acknowledge the support from team of TIFR-BARC Pelletron Linac Facility and the cooperation of the INGA Collaboration. We acknowledge Prof. I. Ragnarsson for help received regarding CNS.

References

- [1] S. Saha *et al.*, Phys. Rev. C **99**, 054301 (2019).
- [2] B.G. Carlsson, Phys. Rev. C **78**, 034316 (2008) and references therein.
- [3] Y. Zheng *et al.*, Phys. Rev. C **100**, 014325 (2019).
- [4] R. Palit *et al.*, Nucl. Instrum. Methods Phys. Res., Sect. A **680**, 90 (2012).
- [5] D.C. Radford, Nucl. Instrum. Methods A **361**, 297 (1995).
- [6] A. V. Afansjev *et al.*, Phys. Rep. **322**, 1 (1999), and references therein.
- [7] T. Bengtsson and I. Ragnarsson, Nucl. Phys. A **436**, 14 (1985) and references therein.